

Seismic and tsunami fragility of industries, revealed by the 2011 Tohoku-oki earthquake

KUWAHARA, Yasuto^{1*} ; HASEGAWA, Isao¹ ; YOSHIMI, Masayuki¹ ; NAMEGAYA, Yuichi¹ ; HORIKAWA, Haruo¹ ; NAKAI, Misato¹ ; MASUDA, Satoru²

¹AIST, GSJ, ²Graduate school of Economics and Management, Tohoku University.

We have developed seismic and tsunami fragility curves of industries by using damage data of industrial companies, estimated strong motions and estimated tsunami heights of the 2011 Tohoku-oki earthquake. The damage data were obtained from 7,019 industrial companies through inquiry surveys by the Regional Innovation Research Center of Tohoku University. As a damage level indicator for each company, we introduced a ratio of an economical damage of physical fixed assets excluding lands to previous balance of the physical fixed assets. The estimated strong motions of the 2011 Tohoku-oki earthquake at all the sites of the companies were from the database of the so-called QuiQuake system (Quick estimation system for shaking maps triggered by observation records) operated by the National Institute of Advanced Industrial Science and Technology (AIST). It is noted that the estimated data were obtained by taking account of seismic local site effects and the actually observed ones. The tsunami height data at each site of the company were obtained by interpolating the confirmed data compiled by the 2011 Tohoku Earthquake Tsunami Joint Survey Group (2013). It is found that a frequency-damage level distribution for each seismic intensity is well correlated with a binominal distribution where the only parameter characterizing the distribution is an average value of the damage levels in each seismic intensity. The tsunami fragilities are also obtained as a function of the tsunami height in the same way. These fragility curves can be useful not only to estimate economic damages for future huge earthquakes, but also to rapidly assess the damage just after earthquakes.

Keywords: Seismic, Tsunami, fragility curve, industry, the 2011 Tohoku-oki earthquake

Compiling the source area data of large earthquakes occurred in Pacific Rim

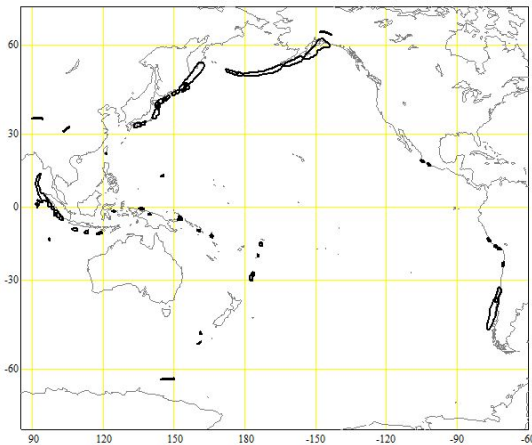
ISHIKAWA, Yuzo^{1*}

¹Y. Ishikawa

The locations of hypocenters were usually plotted by some symbols. This way leads to misunderstand that the earthquake source is the point source. It was caused by the earthquake catalog of which location data were given as a point.

Now, the earthquake source are given by the area obtained by the one month aftershock distributions. Events of which magnitude are larger than 8.0 from 1970, using PDE earthquake catalog. Some large events were added in 20 century. The source areas of large earthquakes occurred in Pacific Rim were digitized.

Keywords: source area, large earthquake, Pacific Rim



A set of characterized earthquake fault models for the probabilistic tsunami hazard assessment in Japan

TOYAMA, Nobuhiko^{1*} ; HIRATA, Kenji¹ ; FUJIWARA, Hiroyuki¹ ; NAKAMURA, Hiromitsu¹ ; MORIKAWA, Nobuyuki¹ ; OSADA, Masaki¹ ; MATSUYAMA, Hisanori² ; KITO, Tadashi²

¹NIED, ²OYO CORPORATION

A set of characterized earthquake fault models are necessary for nation-wide probabilistic tsunami hazard assessment in Japan (Fujiwara et al., 2013; Hirata et al., 2014). It should include all possible earthquakes in future and should take into account various types of uncertainty.

In general, origins of tsunamis include a volcano, a landslide as well as an earthquake, but as the first step we focus on tsunamis that are caused by only earthquakes occurring near Japanese Islands. We introduce our strategy to construct a set of earthquake fault models for tsunami hazard assessment in Japan, showing examples of earthquake fault models along the Japan Trench.

The "Long-term Evaluation of earthquakes from Sanriku-oki to Boso-oki region (2nd edition)" (2011/11/25) by the Headquarters for Earthquake Research Promotion(HERP), Japanese government, defined 8 seismogenic segments along the Japan Trench. Based on these segmentations, we classify tsunamigenic earthquakes into 7 categories as follows; 1)"March 11, 2011 Tohoku earthquake-type" earthquakes, 2) maximum-sized class earthquakes, 3) other large-sized earthquakes, 4) earthquakes occurring in any single segment which HERP assessed its possible magnitude and/or location with recurrence interval, 5) tsunami earthquakes, 6) intra-plate earthquakes with normal faulting, and 7) moderated-sized earthquakes (HERP called this type "earthquakes which we cannot expect its magnitude and size"). HERP assessed earthquake potentials only in categories 1), 4), 5), and 6). To enhance the entirety of tsunami hazard assessment, we newly add the categories 2), 3) and 7), though no previous earthquakes in categories 2), 3), and 7) are known yet. We place earthquake fault on the upper boundary of the subducting Pacific Plate except earthquakes of the category 6).

Seismic moment, M_0 , to a characterized earthquake fault model, is determined by an empirical scaling relation between M_0 and fault area, S . To determine the empirical relation we first make a list of tsunamigenic earthquakes from the data base of "Size of tsunamis around Japan for 1498-2006" (<http://www.eri.u-tokyo.ac.jp/tsunamiMt.html>) by Abe. Next we assign M_0 and S to listed tsunamigenic earthquakes, referring in previous studies (Sato et al., 1989) and then derive an empirical M_0 - S scaling relation for tsunamigenic earthquakes occurred in the area of the Pacific ocean side. There are some previous studies suggesting that rigidity is depth dependent, but we use a constant value of $5 \times 10^{10} (\text{N/m}^2)$ as rigidity.

We introduce inhomogeneity in earthquake fault slip to define "large slip area (LSA)" and "extremely large slip area (ELSA)" by following a characterized ratio of high-slip area to entire fault area (Korenaga et al., 2014). For great earthquakes of $M_w > 8.4$, LSA is allowed to be located 3 patterns for along-trench direction and 3 patterns for trench-normal direction, thus total of 9 basic configurations, for each characterized earthquake fault model. ELSA can be allowed to be located along the upper edge in a LSA when the LSA is located adjoined the trench axis. For large earthquakes with the magnitudes less than ~ 8.3 , that is the category 7), we consider only a LSA at the center of the entire fault area. In this case, variability of possible LSA location is taken into account by introducing an uncertainty value of possible LSA location in process of tsunami hazard curve calculation.

A set of characterized earthquake fault models that we place along the Japan Trench, spans from M_w 7.0 to 9.4 at every 0.1 or 0.2 magnitude intervals. Total number of the models along the Japan Trench reaches more than 1800. It takes whole three months to complete non-linear tsunami simulations for all characterized earthquake fault models.

This study was done as a part of "Tsunami hazard assessment project for Japan" in NIED.

Keywords: tsunami hazard assessment, probability, characterized earthquake fault model

Tsunami hazard assessment project in Japan

HIRATA, Kenji^{1*}; FUJIWARA, Hiroyuki¹; NAKAMURA, Hiromitsu¹; OSADA, Masaki¹; OHSUMI, Tsuneo¹; MORIKAWA, Nobuyuki¹; KAWAI, Shin'ichi¹; AOI, Shin¹; YAMAMOTO, Naotaka¹; MATSUYAMA, Hisanori²; TOYAMA, Nobuhiko²; KITOH, Tadashi²; MURASHIMA, Yoichi³; MURATA, Yasuhiro³; INOUE, Takuya³; SAITO, Ryu³; AKIYAMA, Shi'ichi⁴; KORENAGA, Mariko⁴; ABE, Yuta⁴; HASHIMOTO, Norihiko⁴

¹NIED, ²OYO, ³KKC, ⁴CTC

Tsunami hazard assessment (THA) is the most important information to take effective measures against possible tsunami attacks in future. After the national tragedy caused by the 11st March 2011 Tohoku earthquake (Mw9.0), NIED started a research project regarding TSA in Japan to support various kind of measures by sectors such as local governments, life-line companies, etc (Fujiwara et al., 2013, JpGU). Our research project consists of two components; (A) a research of probabilistic tsunami hazard assessments (PTHA) in which we consider all of possible tsunamis that may affect coastal regions in future and (B) a research to forecast coastal tsunami heights and inundation flow depths based on specified earthquake scenarios.

In the research (A) of PTHA, we began working on subjects of (1) nation-wide probabilistic tsunami hazard assessment (NW-PTHA) and (2) detailed probabilistic tsunami hazard assessment for a specific region (DPTHASR). Outlines of (1) NWPHTA are as follows; (i) we consider all of possible earthquakes in future including earthquakes that the Headquarters for Earthquake Research Promotion (HERP), Japanese Government, already assessed. (ii) We construct a set of simplified earthquake fault models, called "characterized earthquake fault models (CEFMs)", for all of the earthquakes mentioned above by following prescribed rules (Toyama et al., 2014, JpGU; Korenaga et al., 2014, JpGU). (iii) We solve a non-linear long wave equation, using staggered leap-frog, finite difference method (FDM), including inundation calculation as coastal boundary condition, over a nesting grid system with the minimum grid size of 50 meters, to calculate tsunamis for each of initial water surface distributions (under research for initial water surface calculation by Akiyama et al., 2014, JpGU) generated from a large number of the CEFMs. (iv) Finally we integrate information about coastal tsunami heights from the numerous CEFMs to get nation-wide tsunami hazard curves, defining excess probability, for coastal tsunami heights, incorporating uncertainties inherent in tsunami forward calculation and earthquake fault slip heterogeneity (Abe et al., 2014, JpGU). In the present step we are revising a prototype of NWPHTA in the case where possible tsunami sources are located along the Japan Trench as well as we are constructing a set of CEFMs in the case where possible tsunami sources are located along the Nankai Trough.

As for the research of (2) DPTHASR, we are going to develop new methods to assess inundation probability and inundation time, etc., through tsunami inundation simulations for a set of CEFMs using the same FDM over a nesting grid system with the minimum grid size of 10 meters including information of seawalls and breakwaters. Some of results from DPTHASR will be represented in a similar format of "Karte" (medical chart) to help understandings of tsunami hazard information by residents. In the present step, we are constructing a new method to assess probabilistic inundation depth distribution along with calculation of hazard curves for inundation depth at specified points on land (Saito et al., 2014, JpGU).

In the research (B), we are planning to construct a deterministic method to forecast coastal tsunami heights, inundation area and depth, etc. in specified sites in the scenarios that possible maximum-sized tsunamis strike there. These deterministic forecasts should be examined through comparisons with tsunami deposits distribution, historical materials, and instrument records.

Also, we are making a lot of effort to utilize probabilistic and deterministic tsunami hazard information by investigating actual usages of domestic/oversea tsunami hazard information (Osada et al., 2014, JpGU) and by investigating opinions and ideas from persons-in-charge of measures by local governments for tsunami disasters thorough questionnaire surveys with direct interviews (Ohsumi et al., 2014, JpGU).

This work partially functions to support activities of HERP.

Keywords: tsunami, hazard assessment, probability, scenario-type tsunami forecast, hazard map, utilization

G-EVER Earthquake and Volcanic Eruption Risk Management Activities and Asia-Pacific Region Hazard Mapping Project

TAKARADA, Shinji^{1*} ; ISHIKAWA, Yuzo¹ ; BANDIBAS, Joel¹ ; G-EVER, Promotion team¹

¹Geological Survey of Japan, AIST

The Asia-Pacific Region Global Earthquake and Volcanic Eruption Risk Management (G-EVER) Consortium among the geo-hazard research institutes in the Asia-Pacific region was established in 2012. G-EVER aims to formulate strategies to reduce the risks caused by earthquakes, tsunamis and volcanic eruptions worldwide. The First Workshop on Asia-Pacific Region Global Earthquake and Volcanic Eruption Risk Management (G-EVER1) was held in Tsukuba, Japan from February 22 to 24, 2012. During the workshop, the G-EVER1 accord was approved by the participants. The Accord consists of 10 recommendations such as; enhancing collaboration, sharing of resources, and making information of the risks of earthquakes and volcanic eruptions freely available and understandable. The G-EVER Hub website was setup to promote the exchange of information and knowledge about volcanic and seismic hazards among Asia-Pacific countries. Establishing or endorsing standards on data sharing and analytical methods is important to promote data and analyses results sharing. The major activities of G-EVER include participation in global risk reduction efforts such as the Integrated Research on Disaster Risk (IRDR) Program, Global Earthquake Model (GEM) and Global Volcanic Model (GVM). The 2nd G-EVER International Symposium and the 1st IUGS&SCJ International Workshop on Natural Hazards was held in Sendai, Tohoku Japan on October 19-20, 2013. We endorsed Sendai Agreement during the symposium (<http://g-ever.org/en/sendai/>). Several G-EVER Working Groups and projects were proposed such as; (1) Risk mitigation of large-scale earthquakes WG, (2) Risk mitigation of large-scale volcanic eruptions WG, (3) Next-generation volcanic hazard assessment WG, and (4) Asia-Pacific region earthquake and volcanic hazard mapping project.

The Asia-Pacific region earthquake and volcanic hazard mapping project aims to make an advanced online information system that provides past and recent earthquake and volcanic eruption information (e.g. age, location, scale, affected areas and fatalities) and risk assessment tools for earthquake and volcanic eruption hazards. A printed map will also be published as the new version of the Eastern Asia Geological Hazard Map of the Commission for the Geological Map of the World (CGMW). The online hazard mapping system will provide useful information about earthquake and volcanic hazards in an interactive and user-friendly interface. Past and recent large-scale earthquakes and volcanic eruptions, tsunami inundation areas, and active faults distributions will be shown on the map. Links to major earthquakes and volcanic eruptions databases will be available in the system. The earthquake and volcanic eruption hazard mapping project will be implemented with the cooperation of major research institutes and organization in the Asia-Pacific region such as PHIVOLCS, CVGHM, GNS Science, EOS, USGS and CCOP.

Keywords: Earthquake, Volcano, Risk, Hazard, Hazard Map, Asia Pacific

Observing Schumann Resonance by demodulating High Frequency Waves

CAO, Bingxia^{1*}; ZHOU, Hongjuan¹

¹Harbin Institute of Technology at Weihai

The limited dimensions of the Earth cause the waveguide between the surface of the Earth and the conductive ionosphere to act as a resonant cavity for electromagnetic waves in the ELF band so that Schumann Resonance (SR) occurs there. It has been suggested that SR may be used to monitor global temperature variations. SR has been used to study the lower ionosphere on Earth and suggested as one way to explore the lower ionosphere on celestial bodies. A new field of interest using SR is related to short-term earthquake prediction. The manmade noises in the ELF band was a problem for observing. A new way to observe SR based on cross-modulation in the low ionosphere is discussed.

The effect of cross-modulation was established by Yampolski et al. between SR and HF signals experimentally. The HF signals called Round-the-world signals (RWS) and large antenna arrays of the radio telescope UTR-2 were used. But the problem is whether the SR can be seen only with a simple antenna. If the answer is yes, we have a new measurement method for SR.

The HF-SR multiple mode nonlinear interaction theory is researched based on the basic theory model established. In the multiple interaction mode theory, the modulation depth is affected by electromagnetic wave phase in the nonlinear effect. Before the experiment, a lot of simulation experiments and theoretical research are carried out, including Schumann Resonance global distribution simulation and multi-mode interaction of HF-SR theory etc.. One simpler half wave cross dipole antenna is used to receive the time service signal of China called BPM. And in the demodulation spectrum of BPM, the first 4 order resonance peaks of the SR are obtained successfully, respectively on 7.5Hz, 14Hz, 20Hz and 26Hz.

The electric field distributions and phase variations of the first 3 order peaks of Schumann Resonance in the earth ionosphere cavity are obtained through a series of SR distributed simulation experiments. The result shows that in the same phase region, the phase of SR only depends on time. At the same time all the points have the same vibration phase. Two points have 180 degree difference phase after a phase mutation point.

The actual multi interaction mode effect between RWS and SR is uncertain. It may change with the propagation conditions. The modulation depth can not be increased significantly in the multiple interaction effects of HF wave and SR propagate around the globe. The main reason is the high frequency wave goes through the the phase jump points of Schumann Resonance. The final depth of modulation in the Yampolski experiment is about 0.7-3.5 times to the modulation depth of single interaction.

RWS goes through around the earth. But the modulation depth of RWS and SR nonlinear effect is not significantly far greater than that of 1 jump value because of the path length growth.

Using the RWS signal, greater modulation than short reception, for example, 1 hop, can be obtained. But due to the SR wave distribution in the earth ionosphere cavity, the value is less than the direct summation of each modulation results. That is to say, high frequency electromagnetic wave propagates around the earth for nearly a circle. It is modulation result with SR dose not significantly increase compared with that of the obtained by ionospheric reflection arrive at the receiving station.

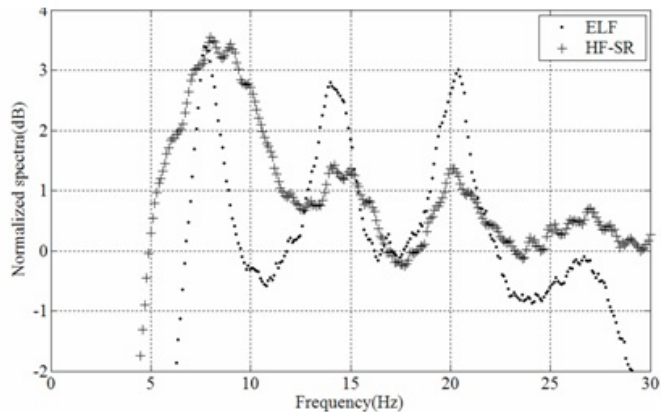
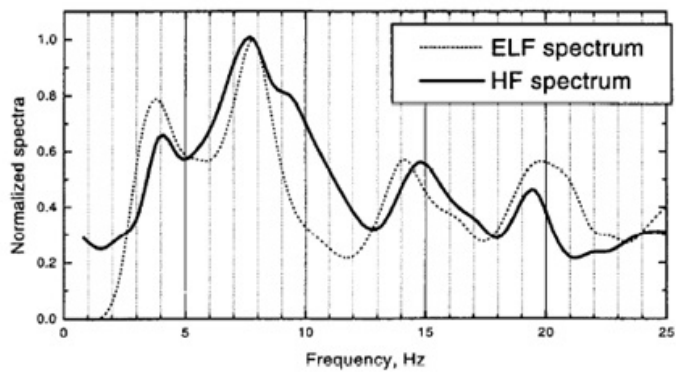
According to the new theory of HF-SR interaction, a receiving station was established. The system receives the BPM time service signals from the National Time Service Center in PuCheng, 1160 km away from the receiver. The carrier frequency is 10 MHz. By demodulating the BPM signal, the first 4 order peaks of SR are obtained. Maybe it is a new way for SR observing.

Keywords: earth ionosphere cavity, Schumann Resonance, nonlinear effect, high frequency wave

HDS28-06

Room:312

Time:May 1 17:30-17:45



Influence of microtopography in lowland to tsunami disaster of 2011 Tohoku Earthquake

IKARI, Kazuya^{1*} ; NARAMA, Chiyuki²

¹Graduate School of Science & Technology, Niigata University, ²Faculty of Science, Niigata University

The earthquake (magnitude 9.0) on Mar 11, 2011 in Tohoku, Japan triggered the terrible destructive tsunami, striking the eastern coastal region of Japan. Although residents in valley bottom plain of the Sanriku Coast (ria coast) have a refuge area around hills, residents in Sendai Plain (meander plain of lowland) had to go inland in order to escape tsunami. The lowland such as Sendai Plain is very vulnerable to tsunami. However, Building damages differed among the Sendai Plain. This study evaluated the influence of landform in lowland of Sendai Plain to tsunami disaster.

The Sendai plain is meander plain of lowland (0-3m asl.), including beach ridges and inter-ridge march of ridged beach plain, and natural levees along present and meander scars. Three beach ridges are developed along the coast. Relative height of present beach ridge is 3-5m, and inner two beach ridges are 1-2m.

We classified three damage-categories (flow out, destroy, and remain) to individual buildings in tsunami inundation area of the Sendai Plain, based on interpretation of aerial-photographs on 2011 and Google Earth satellite image 2012. In addition, we made a GIS data of utility pole, flattened tide protection forest, driftwood, tsunami scratch in Sendai Plain, to know flow directions of tsunami and distribution of woods.

Building damages in the Sendai plain show >80% of buildings flowed out within 1km area from the coast. Remaining buildings are located on ridged beaches with 1-2m high. Driftwood and rubble had stopped on the near side of beach ridges and highway embankment. Tsunami flow was concentrated in the inter-ridge march or small stream channels. Around the Abukuma River, buildings under cut slope received tsunami damage, and slip-off slope side was safety. In lowland plain, we clarified microtopography with 1-2m relative height reduced tsunami damages around inland side area (>1km) from the coast.

Keywords: 2011 Tohoku Earthquake, tsunami, Sendai Plain, lowland, microtopography, aerial-photographs

Eruptive Sequence of Rinjani Caldera, 13th Century, Lombok, Indonesia

FURUKAWA, Ryuta^{1*}; TAKADA, Akira¹; NASUTION, Asnawir²; TAUFIQURROHMAN, Roni³

¹Geological Survey of Japan, AIST, ²Institute Technology of Bandung, ³Center for Volcanology and Geological Hazard Mitigation

Rinjani Volcanic Complex located at northern part Lombok Island is centered by a large stratovolcano, Rinjani volcano, which is the volume of 100 km³ and 3726m high (Nasution et al., 2003). A caldera of 6x8 km in diameter lies western side of the summit formed at mid-13th century (Nasution et al., 2010; Lavigne et al., 2013). Sequence of the caldera forming eruption is reconstructed from original stratigraphy of eruptive deposits and consists of 6 phases with no prominent time interval between them. Phase 1 is a small phreatic eruption produced thin ash fall bed only occurs proximal of the summit. Phase 2 is large plinian eruption dispersed pumice lapilli to western side and extending to adjacent islands. Pumice lapilli become finer and lithic fragments increase upward in the fall bed. Phase 3 is defined by widely extending pyroclastic flow deposit consists of vaguely bedded unsorted ash with subordinating rounded pumice lapilli. Its thickness varies from several to 50 cm especially thickens local topographic depression and eroding underlying pumice fall bed. This deposit extends more than 50 km from the probable source and reached Gili Island isolated by ocean suggesting extremely dilute pyroclastic flow possibly caused by plinian eruption column collapse from high altitude. Phase 4 is unstable plinian eruption implied by graded pumice lapilli bed intercalated by multiple thin ash beds. Phase 5 is characterized by enormous pyroclastic flow effusion resulting thick and massive pumiceous lapilli tuffs extending more than 30 km from the source. Proximally fines depleted lithic breccia including andesite lavas and minor amount of granodiorite are interbedded with massive pumiceous lapilli tuff. Thickly stratified lapilli tuff beds exposes along the coastline suggest the pyroclastic flow caused the secondary explosions and formed littoral cone at the ocean entry. Phase 6 is last plinian eruption dispersed pumice fall of limited extent which is smaller than preceding plinian phases 2 and 4. Petrological analysis shows magma composition changes between phase 3 and 4 suggesting formation of new vent or widening pre-existing vent eventually causes the caldera formation.

Keywords: volcano, caldera, pyroclastic flow, Indonesia, ash, icecore